Hindawi
Advances in Civil Engineering
Volume 2022, Article ID 7391622, 9 pages
https://doi.org/10.1155/2022/7391622

Research Article

Effect of Size on the Stability of Narrow Foundation Pits

Caihao He,[1] Yi Lu,[2] and Yanlu Yang[3]

[1]*Jingzhou University, Jingzhou 434000, China*
[2]*School of Urban Construction, Yangtze University, Jingzhou 434020, China*
[3]*Sinopec Yantai LNG Co., Ltd., Yantai 264000, China*

Correspondence should be addressed to Yi Lu; 202072710@yangtzeu.edu.cn

Received 4 May 2022; Revised 25 November 2022; Accepted 15 December 2022; Published 30 December 2022

Academic Editor: Zhiguo Zhang

The traditional design method for narrow foundation pits ignores size effects. Engineering practice shows that this is too conservative and causes large-scale waste. In this study, with the help of ABAQUS finite element software, retaining-structure models in semi-infinite and infinite elastic space are used to simulate the mechanical performances of pile-supported structures under different combinations of excavation depth, retaining pile-embedded depth, and excavation width. Furthermore, based on antioverturning stability theory and circular slip theory, the intrinsic relationship among these variables and their effects on the stability of excavation is analysed. Finally, based on the restraint effect of retaining structures on the soil below the pit bottom under actual working conditions, critical width is determined and used to classify foundation pits. Moreover, the applicability of existing codes is discussed. These results can improve the design and construction of narrow excavations, benefitting the construction industry and society in general.

1. Introduction

Currently, the trend of urban construction in China towards underground space is becoming more and more obvious; the importance of tube-tunnel and tube-network engineering is increasing daily. In such projects, the foundation pit is typically a long trench, and the width of which is small in comparison to its depth; supporting structures on both sides of the foundation pit are close to each other.

In practice, this kind of foundation pit is called the foundation trench, and the dependence of foundation pit deformation and stability on geometrical factors such as width, length, and depth is called the "size effect" [1]. By comparing practice with theory, Zeng and Yang [2] found that foundation pit width has a significant impact on uplift stability. Investigating antiuplift stability, Huang and Qin [3] found that the safety factor calculated by the foundation-bearing capacity model without considering the width term is too large. By comparing software simulation results, Wang and Zhang [4] found that the opposite retaining wall of a narrow foundation pit has a restrictive effect on the pit's antiuplift stability. Therefore, the trapezoidal failure mode is proposed, which well considered the influence of the width of foundation pit on the antiuplift stability of narrow and long foundation pit. Qi [5] considered the influence of foundation pit width on the antiuplift safety factor K at the bottom of the foundation pit. As the pit width decreases, K increases at an increasingly fast rate. Qin et al. [6] found that increasing the depth-to-width ratio reduces the antiuplift stability coefficient. Wang et al. [7] proposed a deformation mechanism for narrow foundation pits based on the Terzaghi mechanism using the deformation increment of the Ricken distribution function and calculated K considering the geometric size of the foundation pit. Parameter analysis and case verification showed that the size effect is more obvious at smaller width-to-depth ratios and that the antiuplift safety coefficient is also larger. Xiao et al. [8] analysed and processed field-monitoring data from 92 foundation-pit excavations with different widths in soft soil areas of China, finding that narrow foundation pits showed an obvious size effect due to the influence of the opposite retaining wall. Ge [9] studied support structure deformation after the excavation of foundation pits with different length-to-width and width-to-depth ratios by

numerical simulation. Narrow underground railway foundation pits exhibited a spatial effect: the displacement of the long side changed significantly. Previous studies have shown that the shape and size of the foundation pit have a significant influence on deformation and stability. Wang [10, 11] proposed an improved algorithm considering these factors. In practical engineering, it is well established that narrow foundation pits are more stable. For example, as long as a transverse plate support is adopted, the retaining structure of a general shallow trench can maintain the stability of the foundation pit without insertion of soil below the pit bottom [12]. Research suggests that this is because the retaining structures on both sides of the trench restrain the pit bottom soil.

When the foundation pit cannot meet stability specifications, the embedded depth of supporting piles is usually increased. However, for a narrow foundation pit, utilising the size effect should be given priority, because the existing specification algorithms assume that the foundation pit is very wide and only take a one-sided retaining structure and the soil in the passive zone as the research objects. As a result, the influence of foundation pit width is not reflected in standard stability analysis by normative methods [12], resulting in great design waste. Some scholars have carried out fruitful research work, combined with the finite element numerical model, and analysed the narrow instability characteristics of the foundation pit. Using Coulomb–Wedge analysis, Ying et al. [13] modelled the passive earth pressure of the translational rigid retaining wall of a narrow foundation pit and deduced analytical formulas for the sliding crack surface inclination and passive earth pressure coefficient in a passive limit state. Zheng et al. [14] analysed the influence of the length and flexural strength of the retaining structure on the failure mode and safety factor; they proposed that the sliding surface touching the enclosure structure should be used to distinguish the wide and narrow foundation pits. Compared with a wide foundation pit, a narrow foundation pit has more advantages in stability because of its smaller size [15].

When applying a circular sliding mode, the sliding surface of a narrow foundation pit requires spatial effect corrections to improve the safety factor. Wang [16] simplified the uplift deformation of foundation pit as the plastic zone expansion problem caused by the load applied to the bottom of the pit on the elastic half space.444 At the same time, substantial progress has been made in developing an antioverturning stability algorithm [17, 18] that incorporates the foundation pit width into an antiuplift stability formula based on the circular arc-sliding mode [12, 19–22] and the foundation-bearing capacity mode [23]. In addition, Zhang et al. [24] and Liu et al. [21] have studied the uplift failure mechanism of long and narrow foundation pits via centrifugal model tests. Such studies have rarely used numerical analysis to verify the size effect and classify foundation pits under realistic conditions. Hosseinzadeh and Joosse [25–28] studied the influence of soil coupling in the passive area of foundation pits on the stability of foundation pits, calculated the coefficient of passive earth pressure and active earth pressure, and introduced the strengthening factor of passive earth pressure to optimise the embedding depth of the envelope structure.

In the present study, finite element simulations are conducted using standard algorithms that reflect actual working conditions. A semi-infinite-medium elastic model not considering the size effect and an infinite-medium elastic model considering the size effect are created to simulate the mechanical characteristics of foundation pits under various working conditions. Combining the numerical results with results in the literature, this study reveals the essential mechanism of the foundation pit size effect and shows the theoretical reasons for the design waste in existing algorithms. Finally, foundation pits are classified according to their critical width, which can be used to optimise supporting structures.

2. Analysis of Mechanical Deformation Characteristics of a Narrow Foundation Pit

In the model, semi-infinite and infinite elastic spaces are used to simulate unilateral structures and analyse the overall situation. Given the excavation depth H, the embedded depth D of the supporting pile, and the variable foundation pit width B, the main shape variables and stress values may be extracted from the simulation results. The critical width of the foundation pit is determined by a single parameter depending on B: when the parameter is greater than the critical width, a semi-infinite elastic medium is used for the analysis; when it is less, an infinite one is used, conforming to the stress characteristics of the narrow foundation pit. When the parameter is equal to the critical width, the result is the same for both cases.

The usual support method for a foundation trench was assumed: a steel sheet pile (type IV Larsen) and one support (a seamless steel pipe with a diameter of 609 mm and a wall thickness of 12 mm). The construction process simulated an actual-layered excavation. The U-shaped steel sheet pile was converted into rectangular sections with equivalent moments of inertia. The Mohr–Coulomb plastic model was used for soil; the supporting structure was assumed to be elastic. For simplicity, only a single soil layer is considered and silty clay representative in Jingzhou area is selected. Its physical and mechanical parameters were selected on the basis of a geological exploration report. The analysis steps during modelling were set according to the actual construction process: the steel sheet pile was applied, and the steel pipe support was arranged after the corresponding soil layer was excavated. In the process of balancing in situ stress, the supporting structural unit was "killed"; it was then activated for the analysis that ensured the functioning of the subsequent support [29]. The contact between the steel sheet pile and soil was realized by binding constraints. The horizontal displacement of the left and right boundaries of the model was limited, and the bottom surface was constrained by fixed supports. The boundary constraints of the model are shown in Figure 1. The material parameters in the modelling process are shown in Table 1.

The analysis was performed using ABAQUS finite element software. The grid was unevenly divided to improve

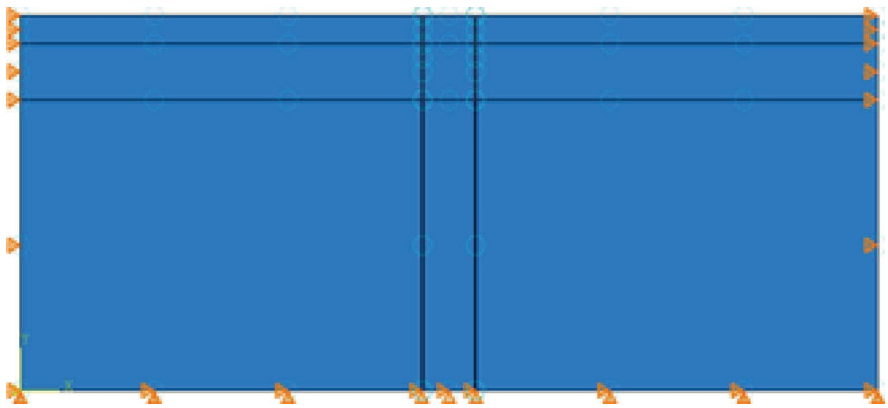

Figure 1: Boundary constraint diagram of the model.

Table 1: Physical and mechanical material parameters.

Material	ρ (kg·m^{-3})	E (kPa)	μ	φ (°)	c (kPa)
Silty clay	1800	1×10^4	0.3	20	19
Steel pipe support	7800	2×10^8	0.3	—	—
Sheet pile	7800	2×10^8	0.3	—	—

the accuracy and efficiency of the plane-strain calculations. The division of the grid should follow the principles of regularity, orderliness, and appropriate density, but to reduce the computational workload and facilitate convergence, it is permissible to increase the mesh density for more significant parts [30]. The size of this model was 100 m × 50 m. To meet the requirements of the two-dimensional model analysis area, the excavation boundary of the foundation pit is extended outward by more than twice the excavation depth and the bottom of the foundation pit is more than twice the excavation depth [31]. A total of 1536 units and 1617 nodes were divided, and the type of grid unit was CPE4R. When arranging seeds, the global seeds were arranged as 3, and the seeds of key parts were coded as 1. The mesh division diagram of the model is shown in Figure 2.

Three common length specifications (9, 12, and 15 m) were selected for steel sheet piles. Based on the actual project, three groups of numerical simulation tests were set (Table 2); the working conditions were numbered in the order of D from small to large. The simulation results for the equivalent plastic strain of a narrow foundation pit in a semi-infinite and infinite elastic medium are shown in Figure 3. Considering the small size of foundation pit in engineering practice, in order to display the failure mechanism clearly and intuitively, we took the working conditions as follows: $H = 10$ m, $B = 14$ m, and $D = 15$ m. The simulation results are shown in Figures 4 and 5.

It can be seen from Figure 3(b) that for a narrow foundation pit, the strain distribution of soil in the passive zone is similar under both conditions. The soil close to the base near the supporting piles on both sides produces the maximum equivalent plastic strain; this weak area is prone to stress under deformation during construction. However, the stress change in the case of the infinite space is small. For

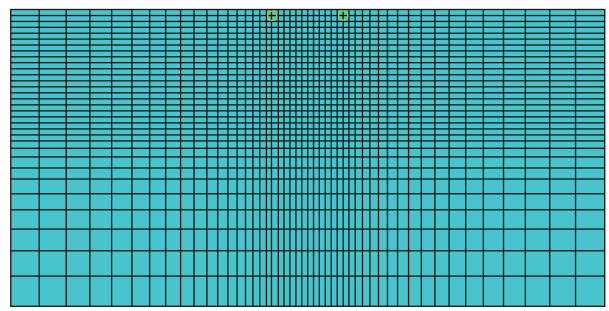

Figure 2: Schematic diagram of the meshing of the model.

observational convenience, a working condition with large size was selected. At this time, the foundation pit's width was close to critical, so the difference between the two cases was not significant. Ground overload and excavation cause a large pressure difference between the interior and exterior of the pit. When the shear strength of soil is exceeded, uplift instability characterized by stress strength failure will occur. As shown in Figure 5(a), the pressure difference forces the active zone on both sides to squeeze the soil in the passive zone and the support pile effectively limits the displacement of the soil outside the pit. The soil below the pit bottom undergoes uniform and small deformation that is significantly less than a maximum deformation of 50 mm at 2 m above the pit bottom (Figure 4), which is mainly due to the lack of internal support near the pit bottom, low stiffness of the support structure, and relative lack of deformation resistance. In Figure 5(b), because of excavation and unloading, the soil in the passive zone can only rise upward after the displacement on both sides is limited. The uplift is largest in the middle of the pit. Under the joint action of the pressure difference and support structure constraints, the soil on both sides has local stress concentrations and maximum equivalent plastic strain. It can be seen from Figure 4 that the top of the supporting pile has a displacement trend outside the foundation pit, whereas the direction of the substructure is opposite. Thus, the foundation pit shows certain "skirting" failure characteristics.

In total, eight quantities, including the axial force of the steel pipe support and the maximum stress and displacement

Table 2: Actual working conditions in simulations.

Excavation depth H (m)	Embedded retaining pile depth D (m)	Foundation pit width B (m)	Bottom support to pit bottom distance d (m)
4	5, 8	2, 4, 6, 8, 10, 12	3
6	3, 6, 9	3, 5, 7, 9, 11, 13	5
8	4, 7	4, 6, 8, 10, 12	7

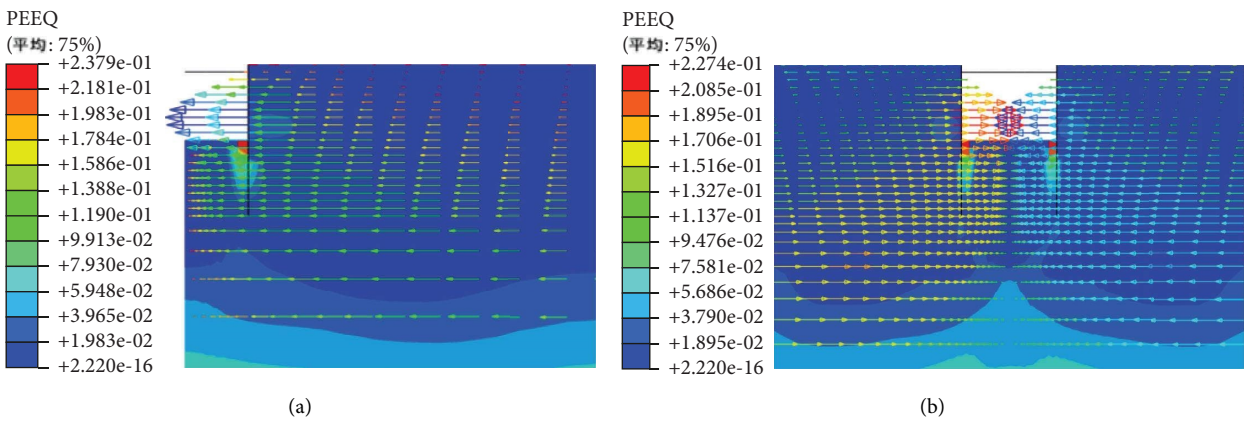

Figure 3: Equivalent plastic strain of a narrow foundation pit for (a) semi-infinite and (b) infinite elastic medium.

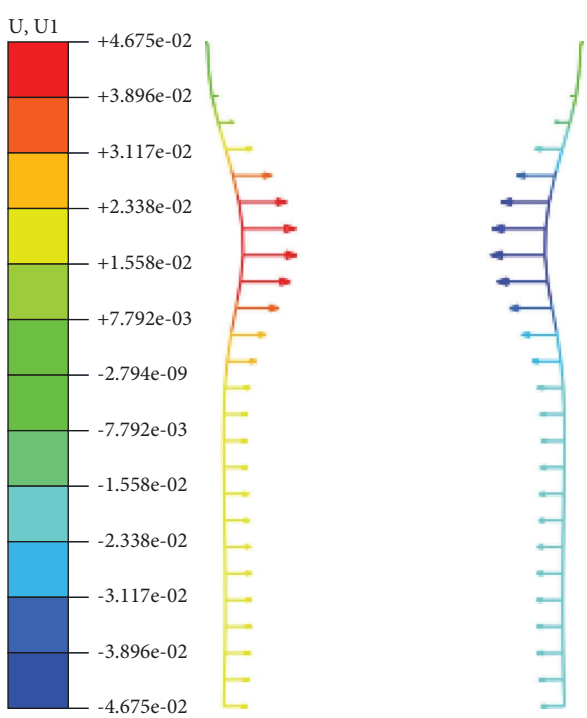

Figure 4: The horizontal displacement of the supporting pile in the case of an infinite elastic space (m).

in the horizontal direction of the steel sheet pile, were extracted from the simulation results. The curve intersections of different parameters under the same working conditions were located. Under the same working condition, the B value at different intersections changed little, fluctuating slightly around a single value. This confirms the existence of critical foundation pit width. The results on each side of the critical value, however, were obviously different. Above the critical width, the two curves were very close and almost coincided, and the existing algorithm was fully applicable. Below it, however, the numerical difference was large; this was increasingly obvious as the pit became narrower. The current method of unilateral structural analysis is unduly conservative, resulting in great waste; the foundation pit size effect should be fully utilised.

3. Study of the Influence of Width on Foundation Pit Stability

When calculating the antioverturning safety factor, it is assumed that, in the event of instability and failure of the foundation pit, the lowest support point is the rotation centre, and the wall bears the active earth pressure on one side of the active zone and the passive earth pressure on one side of the passive zone [32]. According to classical earth pressure theory, when the foundation pit overturns, the soil in the active area will form a slip-surface angle to the vertical direction of $(45^\circ - (\varphi/2))$, where φ is the internal friction angle of the soil; in the passive area, the angle will be $(45^\circ + (\varphi/2))$. Wang [17] discussed in detail the relationship between the formation of the sliding surface in overturning failure and the width of the foundation pit. If α, the relative width of the pit, is defined as the ratio of the excavation width B to the embedded depth D of the supporting pile, it is not difficult to show that, when α satisfies $B/D < \tan(45^\circ + (\varphi/2))$, the sliding surface of overturning failure obtained from Coulomb earth pressure theory will pass through the opposite retaining wall. Thus, the sliding surface cannot be formed as expected because of the restraint, so the

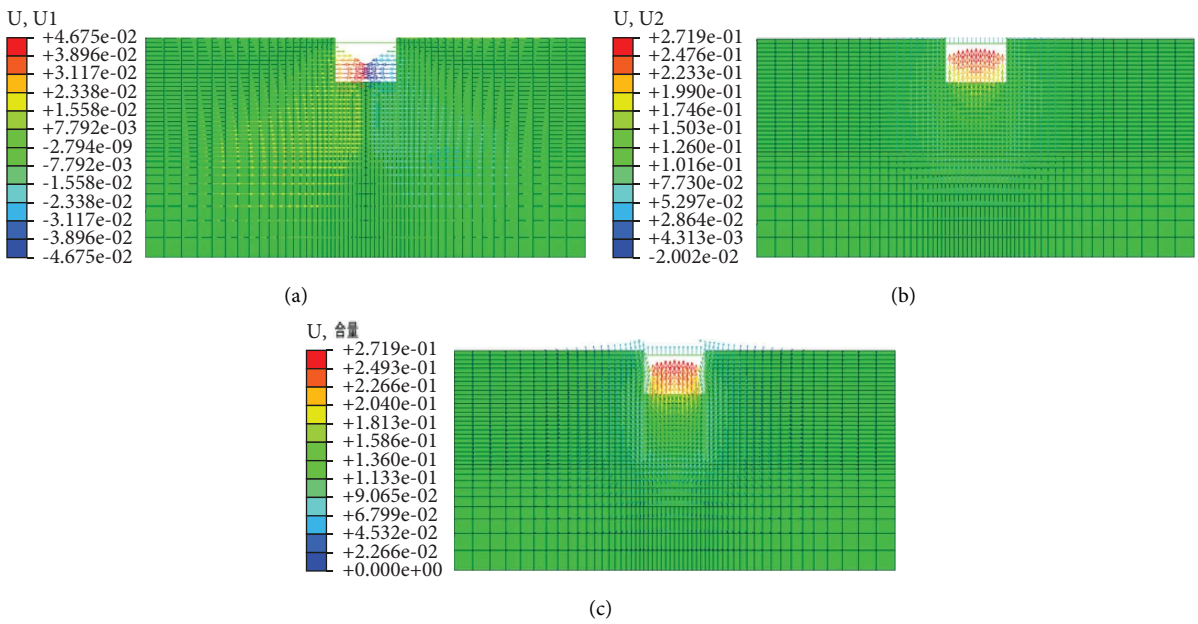

Figure 5: Instability failure mechanism of narrow foundation pits. (a) Horizontal displacement vector. (b) Vertical displacement vector. (c) Displacement sum.

antioverturning stability of the foundation pit is improved. On the other hand, slip-surface formation will not be affected by the opposite retaining wall. Therefore, in practice, when $B/D < \tan(45^\circ + (\varphi/2))$, the restraint due to retaining structures on both sides of the soil at the bottom of the pit should be considered. We can see this more intuitively in the schematic diagram, as shown in Figure 6.

The present standard method of calculating the circular slip stability safety factor of retaining structures assumes that the centre of the slip arc is located at the lowest support elevation. Wang [12] constructed an antiuplift safety factor algorithm considering the width of the foundation pit by making geometric assumptions and conducting physical analysis of the circular slip surface and the position of the centre of the circle. If d is the distance between the lowest support and the pit bottom, then (according to Wang's assumption) the lowest support point is the centre of the circle and the distance $d + D$ from it to the bottom end of the support structure is the radius of circular arc-sliding failure. Obviously, from the geometric relationship, when the width of the foundation pit satisfies $B < \sqrt{(D+d)^2 - d^2}$, the circular slip surface is restrained by the opposite retaining wall. Then, the soil wedge in the passive zone is wedged tightly and cannot slide. Because the coexistence of the two forms of instability, when the foundation pit is damaged, affects the simulation results, the simulation value should be compared with the average theoretical value, and the antisliding stability of the foundation pit is improved. On the contrary, the sliding surface can be formed smoothly. Therefore, when $B < \sqrt{(D+d)^2 - d^2}$, D should be appropriately reduced in the design. We can see this more intuitively in the schematic diagram, as shown in Figure 7.

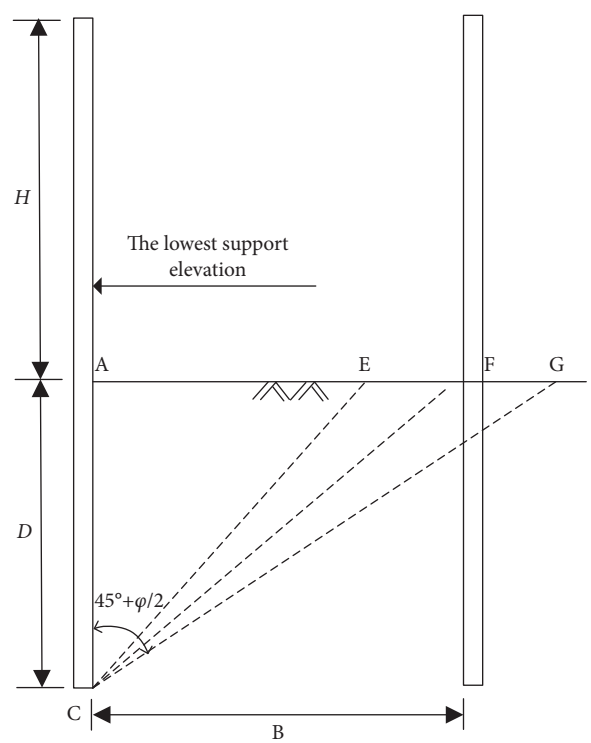

Figure 6: Slip surfaces of soil wedge in the passive area under restraint of retaining structures.

The above analysis leads to different critical widths. Antioverturning theory involves three variables: B, D, and φ. Once the construction site is determined, φ is fixed. Therefore, the critical value of B depends only on D, and the two are related linearly. The graph of B against D is a straight

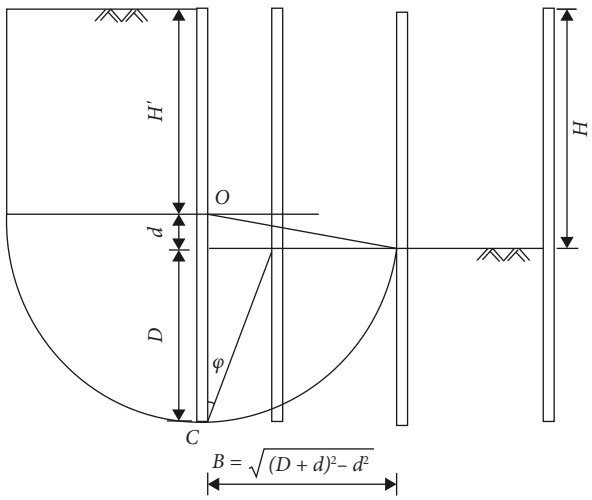

Figure 7: Positions between the retaining wall on the other side and the slip surface.

line passing through the origin in the plane coordinate system.

Circular slip theory, on the other hand, involves three variables: B, D, and d; the critical value of B depends on both D and d. The graph of such a bivariate first-order functional relationship is a surface in a three-dimensional space. Therefore, it is impossible to consider the B-D relationship a single curve. We considered B the dependent variable and the actual working conditions D, φ, and d the independent variable, focusing mainly on the relationship between theoretical and simulated values under various working conditions.

We averaged the intersection positions of different result parameter curves under the same working conditions to eliminate errors and obtain more accurate critical values (see Table 3 and Figure 8) for the critical widths of foundation pits under different working conditions.

As shown in Figure 8, under different working conditions, the jagged lines representing the average simulated and theoretical values were of similar form, and the fluctuations around the average were also very similar. The simulated values were generally less than the average theoretical values. Except in a few cases, the difference between them increased with D. Thus, the finite element model was basically verified, showing that our theoretical analysis of the influence of width on stability is correct; the two expressions for the critical width of foundation pits are reasonable, and a narrow foundation pit is more stable.

To obtain the theoretical critical width from the geometry, it was necessary to make certain assumptions that the lowest support point was the rotation centre of the foundation pit. Whether these assumptions are consistent with the actual failure form of foundation pits remains to be discussed. In addition, in the simulation process, the diversity of contact modes between soil and supporting structure also affects the calculation results, and a variety of factors lead to slight differences between the two.

4. Critical Width and Classification of Foundation Pits

Existing foundation pit specifications fail to consider the restraint effect of the retaining structures on both sides of the soil at the bottom of the pit. When the pit is narrower than the critical width, this effect is significant. Therefore, the determination of the critical width is very important for the design and optimisation of narrow foundation pits. Wang [12, 17] obtained different critical widths from overturning and circular-slip failure theory; however, these values are given only in principle and do not take into account engineering practice. In engineering practice, both types of failure effects coexist when the foundation pit is unstable. In this way, the determination of the critical width of the foundation pit is not only more scientific and reasonable but is also more convenient for engineering application.

The feasible idea is to calculate both theoretical values under actual working conditions and adopt a practical value based on the smaller of the two so that the narrow foundation pit is not damaged. Let B_{QC} and B_{HCmin}, respectively, represent the theoretical values of the antioverturning and the minimum circular slip. The smaller value of the two will be denoted B_{SC}, and the value to be used in practice will be denoted B_{GC}. When D is constant, B_{QC} is only associated with φ; there is no minimum value. The circular slip B_{HC} is only affected by d: the closer the support is to the base, the smaller is the theoretical value of B_{HC}. It is specified in the standard for foundation pits (JGJ120-2012) that the lower support distance should not be less than 3 m; therefore, B_{HCmin} should be taken at $d = 3$ m. Thus, φ alone determines the relative magnitudes of B_{QC} and B_{HCmin}.

Typical silty clay in the Jingzhou area will be used as an example when calculating B_{QC}. The internal friction angle of most soil in the area is concentrated at about 20°, so we assume $\varphi = 20°$. The critical width of foundation pits under actual working conditions is shown in Table 4 and Figure 9 [33].

As shown in Figure 9, the theoretical value of the minimum circular slip under the actual working condition approximately meets the linear relationship $B_{HCmin} = 1.068 \times D + 2.04$. When $\varphi > 30°$, $B_{QC} > B_{HCmin}$ for all $D \in [3, 9]$, so $B_{GC} = B_{SC} = B_{HCmin}$. When $14.5° \leq \varphi \leq 30°$, the point where $B_{QC} = B_{HCmin}$ moves up the straight line $B_{HCmin} = 1.068 \times D + 2.04$ from the point (3, 5.20) to (9, 11.62). Taking $\varphi = 20°$ as an example, B_{QC} and B_{HCmin} intersect at $D = 5.68$ m. When $D \in 3, 5.68]$, Figure 9 shows that $B_{QC} \leq B_{HCmin}$ and that $B_{SC} = B_{QC} = D \times \tan\ (45° + 20°/2)$. However, when $D \in [5.68, 9]$, $B_{HCmin} < B_{QC}$, and therefore, $B_{SC} = B_{HCmin} = 1.068 \times D + 2.04$. In short, when $\varphi = 20°$, the function expression of the real value is shown as follows:

$$B_{SC} = \min\left\{B_{QC}, B_{HC\min}\right\},$$

$$= \begin{cases} D \times \tan\left(\dfrac{45° + 20°}{2}\right), 3\text{m} \leq D \leq 5.68\text{m}, \\ 1.068 \times D + 2.04, 5.68\text{m} < D \leq 9\text{m}. \end{cases} \quad (1)$$

Table 3: Critical width of foundation pit under different working conditions (m).

Working conditions (H, D)	Range of B	Critical width (m)			
		Antioverturning (theory)	Arc slip (theory)	Average of theoretical values	Simulation value
1: ($H=6$, $D=3$)	3~7	4.28	6.25	5.27	5.37
2: ($H=8$, $D=4$)	4~8	5.71	8.49	7.10	7.21
3: ($H=4$, $D=5$)	2~8	7.14	7.42	7.28	6.36
4: ($H=6$, $D=6$)	3~9	8.57	9.80	9.18	7.12
5: ($H=8$, $D=7$)	4~12	10.00	12.12	11.06	10.22
6: ($H=4$, $D=8$)	2~12	11.43	10.58	11.00	8.45
7: ($H=6$, $D=9$)	3~13	12.85	13.08	12.97	9.49

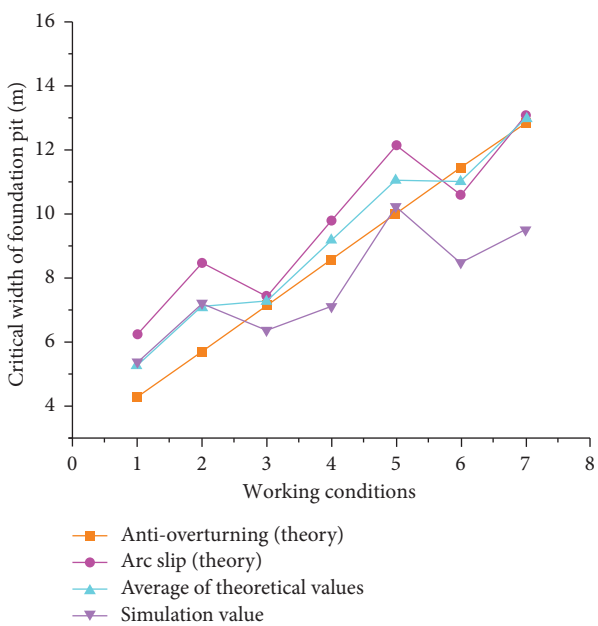

Figure 8: Critical width of foundation pits under different working conditions.

Table 4: Critical width of foundation pits when supporting piles are embedded in different depths (m).

The corresponding width of the two theories	Critical width of foundation pits when supporting piles are embedded in different depths (m)						
	3	4	5	6	7	8	9
B_{QC} ($\varphi=14.5^\circ$)	3.87	5.17	6.46	7.75	9.04	10.33	11.62
B_{QC} ($\varphi=20^\circ$)	4.28	5.71	7.14	8.57	10.00	11.42	12.85
B_{QC} ($\varphi=30^\circ$)	5.20	6.93	8.66	10.39	12.12	13.86	15.59
B_{HCmin}	5.20	6.33	7.42	8.49	9.54	10.58	11.62
B_{SC} ($\varphi=20^\circ$)	4.28	5.71	7.14	8.49	9.54	10.58	11.62
B_{GC} ($\varphi=20^\circ$)	4.28	5.51	6.73	7.95	9.17	10.40	11.62

Such a piecewise function is inconvenient for applications. Instead, we construct the purple line shown in the figure, which connects the point (3, 3tan ($45^\circ+20^\circ/2$)) with the point (9, 11.6), for the engineering application value of linear equations and keep a safe reserve. The equation of the line for the case $\varphi=20^\circ$ is $B_{GC}=1.223\times D+0.62$. Generally, for any φ in the interval [14.5°, 30°], the position of (3, 3tan ($45^\circ+\varphi/2$)) changes, and therefore, the equation of B_{GC} becomes $B_{GC}=[1.94-0.5\tan(45^\circ+\varphi/2)]\times D+4.5\tan(45^\circ+\varphi/2)-5.81$. When $0^\circ<\varphi<14.5^\circ$, Figure 9 shows that $B_{QC}<B_{HCmin}$ for all $D\in[3, 9]$ so that $B_{GC}=B_{SC}=B_{QC}=D\tan(45^\circ+\varphi/2)$.

By considering the two forms of instability, overturning failure and circular slip failure, under actual working conditions and taking the smaller value, the practical critical width of the foundation pit has been obtained. This can be the basis of a practical classification of foundation pits, depending on the width B, pile depth D, and internal friction angle of soil at the bottom of the pit φ. We define a "narrow" pit as the one satisfying Equation (2). When Equation (2) holds, the restraint effect of retaining structures on both sides of the soil at the bottom of the pit should be considered. Otherwise, the foundation pit is classified as "wide," and the standard algorithm is fully applicable.

$$B<\begin{cases}1.068\times D+2.04, 30^\circ<\varphi, D\in[3,9],\\ 1.94-0.5\tan\left(\frac{\pi}{4}+\frac{\varphi}{2}\right)-5.81, 14.5^\circ\le 30^\circ, D\in[3,9]\\ D\times\tan\left(\frac{\pi}{4}+\frac{\varphi}{2}\right), 0^\circ<\varphi<14.5^\circ, D\in[3,9].\end{cases}, \tag{2}$$

When determining the critical width of the foundation pit, not only the provisions on the insertion ratio of the retaining structure in the standard must be considered but also the principles of feasibility and economy. For example, when $H=4$ m, one can theoretically make $D=4$ m, but this would be wasteful and impractical. Therefore, the value range $3\,\text{m}\le D\le 9\,\text{m}$ can meet almost all the needs of practical engineering. The critical width given is only related to D and φ; the type of supporting pile has no influence on it, and the excavation depth H is not involved. B_{HCmin} is always determined with $d=3$ m. In this way, when D is constant and H changes, there is no consequent change in the critical width, effectively avoiding the problem that the critical width is not uniquely defined for all H. At the same time, it ensures that the foundation pit classification is widely applicable to different combinations of H and D. In fact, a larger H implies a larger D in varying degrees, and B_{HC} cannot take the minimum value, which may increase the

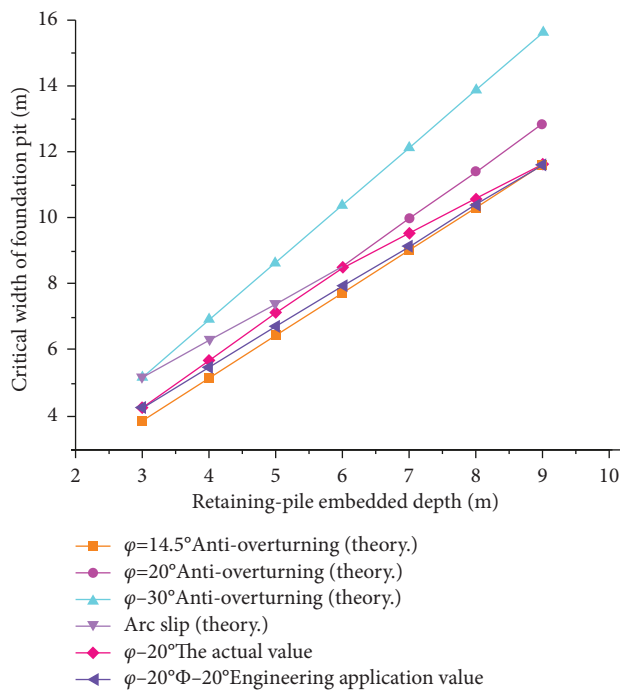

Figure 9: Critical width of foundation pits when supporting piles are embedded in different depths.

critical width slightly. This shows that the critical width obtained by comparing the size of B_{QC} and B_{HCmin} is relatively conservative for ensuring safety: the greater the excavation depth, the more the influence of foundation pit width on stability. Although the foundation pit classification in this study was based on the geological conditions of the Jingzhou area, it is also applicable to other areas. It has certain reference significance for the support design and construction of narrow foundation pits.

5. Conclusions

(1) For a given excavation depth, the foundation pit shows obvious size effects with the change in width. A foundation pit should be classified as "narrow" when the width of the foundation pit is less than the critical width and "wide" when it is greater.

(2) The main factors affecting the stability of a narrow foundation pit are its width, the embedded depth of the supporting pile, and the internal friction angle of the soil, and width is the primary factor. When stability requirements are not met, the embedded depth of the supporting pile should not be unthinkingly increased; instead, the influence of the width on the foundation pit should be considered. In addition, for a foundation pit with poor soil quality, increasing the internal friction angle is also very effective for strengthening the soil in the passive zone and improving the shear strength.

(3) For the support of a narrow foundation pit, the restraint effect of retaining structures on the soil at the bottom of the pit should be fully used to optimise the design and reduce costs.

Data Availability

The data supporting the results of this study are available on request from the corresponding author.

Conflicts of Interest

The authors declare that they have no conflicts of interest.

Acknowledgments

This study was supported by the Open Research Fund of the State Key Laboratory of Geomechanics and Geotechnical Engineering, Institute of Rock and Soil Mechanics, Chinese Academy of Sciences (grant no. Z020013), and the Study on Failure Mechanism and Grouting Reinforcement Technology of Pipe Jacking Excavation in Overlying Water-Rich Sand Layer, Hubei Province (grant no. 2020AC15).

References

[1] C. Y. Ou, D. C. Chiou, and T. S. Wu, "Three-dimensional finite element analysis of deep excavations," *Journal of Geotechnical Engineering*, vol. 122, no. 5, pp. 337–345, 1996.

[2] Q. Zeng and X. Yang, "The calculation model for stability of excavation against upheaval," *Chinese Journal of Geotechnical Engineering*, vol. 18, no. 2, pp. 17–22, 1996.

[3] M. Huang and H. Qin, "Basal stability analysis methods for braced foundation pit," *Chinese Journal of Geotechnical Engineering*, vol. 30, no. 1, pp. 182–186, 2008.

[4] C. Wang and T. Zhang, "The failure patterns and stability analysis of basal heave of long narrow foundation pits," *Science Technology and Engineering*, vol. 17, no. 8, pp. 276–281, 2017.

[5] S. Qi, "Research on stability calculation method of long-narrow groove foundation pit considering spatial effect," *Urban Roads Bridges & Flood Control*, no. 8, p. 283-285+295+31, 2021.

[6] H. Qin, M. Huang, and W. Wang, "Limit analysis method for basal stability of braced excavation against upheaval in heterogeneous soft clay," *Rock and Soil Mechanics*, vol. 29, no. 10, pp. 2719–2724, 2008.

[7] M. Wang, Z. Zeng, and D. Liu, "Upper limit solution for anti-uplift instability of narrow foundation pit under continuous deformation field," *Journal of Chongqing Jianzhu University*, vol. 39, no. 3, pp. 44–50, 2020.

[8] H. J. Xiao, S. H. Zhou, and Y. Y. Sun, "Wall deflection and ground surface settlement due to excavation width and foundation pit classification," *KSCE Journal of Civil Engineering*, vol. 23, no. 4, pp. 1537–1547, 2019.

[9] X. Ge, X. Wang, L. Song, and X. Wang, "Quantitative study on spatial effect of elongated metro foundation pit," *Science Technology and Engineering*, vol. 21, no. 20, pp. 8614–8620, 2021.

[10] H. Wang, "Improvement on safety coefficient of heave-resistant stability of excavations," *Rock and Soil Mechanics*, vol. 35, no. 2, pp. 30–36, 2014.

[11] H. Wang, "A coefficient of heave-resistant stability considering shapes and plane sizes and its application to the stability analysis of shaped excavations," *Chinese Journal of Rock*

Mechanics and Engineering, vol. 34, no. 12, pp. 2559–2571, 2015.

[12] H. Wang, "Size effect of foundation pits and calculation method of safety factor of heave-resistant stability considering excavation width," *Rock and Soil Mechanics*, vol. 37, no. 2, pp. 433–441, 2016.

[13] H. Ying, B. Zheng, and X. Xie, "Study of passive earth pressures against translating rigid retaining walls in narrow excavations," *Rock and Soil Mechanics*, vol. 32, no. 12, pp. 3755–3762, 2011.

[14] G. Zheng, D. Yu, and X. Cheng, "Basal heave stability of wide and narrow excavations considering non-homogeneous features of soft clay," *Chinese Journal of Geotechnical Engineering*, vol. 41, no. 1, pp. 1–4, 2019.

[15] Z. Ding, J. Jin, and T. C. Han, "Analysis of the zoning excavation monitoring data of a narrow and deep foundation pit in a soft soil area," *Journal of Geophysics and Engineering*, vol. 15, no. 4, pp. 1231–1241, 2018.

[16] H. Wang, "Safety factor of heave-resistant stability considering two and three-dimensional size effects of foundation pits," *Chinese Journal of Geotechnical Engineering*, vol. 35, no. 11, pp. 2144–2152, 2013.

[17] H. Wang, "Influence of excavation width on enclosure-structure stability of foundation pits," *China Civil Engineering Journal*, vol. 44, no. 6, pp. 120–126, 2011.

[18] S. Zhao, Z. Chen, and G. Huang, "Effects of foundation pit width on the anti-overturn stability of its support structure underground load," in *Proceedings of the GeoShanghai International Conference*, pp. 488–502, Springer, Singapore, May 2018.

[19] J. Yu, Y. Long, X. Xiao, and X. N. Gong, "Basal stability for narrow foundation pit," *Journal of Zhejiang University (Science Edition)*, vol. 51, no. 11, pp. 2165–2174, 2017.

[20] H. Ying, X. Wang, and J. Zhang, "Analysis on heave-resistant stability considering the effect of excavation width," *Engineering Mechanics*, vol. 35, no. 5, pp. 118–124, 2018.

[21] Y. Liu, C. Xia, and Xu Chen, "Analytical solution and centrifugal test for the optimization of retaining wall insertion depth in narrow foundation pits," *Chinese Journal of Rock Mechanics and Engineering*, vol. 39, no. 3, pp. 593–607, 2020.

[22] X. Cheng, Z. Jie, G. Zheng, Z. Y. Wang, Z. Wang, and X. G. Song, "Research on sliding radius of basal heave failure of excavation in soft soil area," *Journal of Architecture and Civil Engineering*, vol. 38, no. 6, pp. 90–97, 2021.

[23] Y. Chen, "Uplift stability of narrow foundation pits based on Prandtl formula," *Chinese Journal of Geotechnical Engineering*, vol. 41, no. 1, pp. 61–64, 2019.

[24] F. Zhang, J. Li, C. Sun, S. Chang-an, S. Guang-jun, and L. Fei, "Experimental study of basal heave failure mode of narrow-deep foundation pit in soft clay," *Rock and Soil Mechanics*, vol. 37, no. 10, pp. 2748–2754, 2016.

[25] S. Hosseinzadeh and J. F. Joosse, "Design optimisation of retaining walls in narrow trenches using both analytical and numerical methods," *Computers and Geotechnics*, vol. 69, pp. 338–351, 2015.

[26] A. H. Soubra and B. Macuh, "Active and passive earth pressure coefficients by a kinematical approach," *Geotechnical Engineering*, vol. 155, no. 2, pp. 119–131, 2002.

[27] D. Benmeddour, M. Mellas, R. Frank, and A. Mabrouki, "Numerical study of passive and active earth pressures of sands," *Computers and Geotechnics*, vol. 40, pp. 34–44, 2012.

[28] J. S. Shiau, C. E. Augarde, A. V. Lyamin, and S. W. Sloan, "Finite element limit analysis of passive earth resistance in cohesionless soils," *Soils and Foundations*, vol. 48, no. 6, pp. 843–850, 2008.

[29] L. Xu, *FEM Analysis on Dimensional Effect of Foundation Pit*, Tianjin University, Tianjin, China, 2007.

[30] X. Zhang, *Behaviour of Narrow-Deep Excavation in Soft clay Ground*, Zhejiang University, Zhejiang, China, 2012.

[31] T. Feng, G. Qiao, and J. Liu, "Numerical simulation and engineering optimization of diaphragm wall for cantilevered deep foundation pit," *Science Technology and Engineering*, vol. 21, no. 29, pp. 12679–12687, 2021.

[32] J. Liu and X. Hou, *Excavation Engineering Manual*, China Architecture and Building Press, Beijing, China, 1997.

[33] W. Xiao, Y. Lu, Y. Yang, T. Xiao, and Y. Hao, "Stability analysis of narrow foundation pit considering size effect," *Science Technology and Engineering*, vol. 22, no. 10, pp. 4105–4112, 2022.